# Methodology for identification of controller parameters of a diesel generator in islanded grid operation

Claudia Bernecker-Castro[1]*, Johanna Timmermann[1], Drinor Mecinaj[1], Rolf Witzmann[1], Tobias Lechner[2], Sebastian Seifried[2], Michael Finkel[2], Kathrin Schaarschmidt[3] and Steffen Herrmann[4]
[1]Technical University of Munich, Munich, Germany
[2]Augsburg University of Applied Sciences, Augsburg, Germany
[3]LEW Distribution network operator, Augsburg, Germany
[4]AVS Aggregate Construction, Ehingen, Germany
*claudia.bernecker-castro@tum.de

## Abstract

Isolated grid operation has been proposed as a feasible solution in case of long-lasting power blackouts, using the available generation units inside a local area. The availability of reliable generation plant models becomes very important to investigate the new stability margins within an isolated grid. Previous works use simulation models based on simplified controller models [11] or typical controller values [7] found in the literature for stability analysis, which calls into question the applicability of its results in field cases. A more realistic approach, for stability analysis in isolated grids, can be attended by using validated simulation models. However, the absence of general guidelines for parameter validation and optimization makes subsequent analysis difficult. This work proposes a methodology for model validation using measurement data of a synchronous generator powered by a diesel motor, used by a network operator in Germany for emergency power supply during network maintenance. Results show that it is possible to find the best-suited controller parameters, given available standard models for frequency and voltage outputs.

**Keywords** – diesel electric generator, islanded grid, microgrid, particle swarm optimisation (PSO), dynamical modeling, power system stability, frequency stability, voltage stability, controller parameter identification

## 1 Introduction

The increased penetration of inverter-based resources (IBR) has not only changed the structure of the power grid but instead brought challenges to the stable operation of the power system. In Germany, the planned shutdown of nuclear power plants, the high energy prices, and the addition of new loads like heat pumps and electric vehicles into the grid may jeopardize its stability and may increase the possibility of the occurrence of a blackout.

Islanded grids are currently of great research interest since they offer a temporary solution for large-scale power outages [1]. The projects LINDA (Local Island Network supply with Decentralized generation plants) and LINDA 2.0 investigate several aspects regarding isolated grid operation in low and medium-voltage networks using different power sources like a hydro-power plant, a diesel genset, and a battery storage system. The effect of integrating existing rooftop solar power plants in low voltage islanded grids is also studied, without the installation of communication facilities between loads and generators or additional external controllers.

Diesel-electric generators are currently used by network operators, for instance, as an emergency power supply in case of network maintenance. In addition, its potential usage in case of long-lasting power outages is also a research question. Currently, the operating frequency is set so that decentralized generation is not allowed. This is to avoid power fed back into the generator, which physically cannot be absorbed. In Germany, this means the generator operates at a frequency of 51.7 Hz.

A more sustainable operation of this isolated grid should allow the feed-in of existing decentralized generation. Nevertheless, the dynamic interaction between the participating loads and generator units has yet to be determined.

Understanding the dynamics of the components of an isolated grid is essential for the establishment of stability limitations, the development of strategies, and the suggestion of operating improvements. In the case of emergency operation of low-voltage islanded grids, no significant changes in the protection systems are possible. Therefore, factors like peaks and recovery times after a load connection are highly critical to be emulated within a simulation environment. By this, the operating limits of the isolated system are identified and improvements on the generator controller settings can be suggested.

Reliable models of generators and loads are required to predict trustable results of an isolated grid, for instance during transient events. Previous works use simplified controller models [11] or typical controller parameters [7] for stability studies. This calls into question the extent of its applicability in field study cases. Former works also emphasize the frequency behavior [9][10], however, when working in islanded grids as an emergency solution in case of a blackout, it is equally important to consider the voltage behavior. Another challenge is the absence of general guidelines for measurement-based model validation of diesel-electric generators.

This paper proposes an approach to a general, but simple and time-efficient, methodology for the modeling and parameter identification of the most suitable controller values for a 275 kVA diesel electric generator. The parameters are

identified based on measurement data, as described in the third section. The optimization algorithm is used to identify optimal parameter values of the engine governor and exciter models, based on the measured active power and reactive power response of the connected load.
This article is organized as follows: Section II describes the Diesel Electric Generator Model. Section III, the scientific methodology employed in this work for the controller parameter identification is described. Section IV illustrates the validation results for different test cases. Finally, conclusions are met in Section V.

## 2 Diesel Electric Generator Dynamic Model

The network configuration inside the DigSILENT PowerFactory file consists of a generator connected to a load. On the load side, measurement data recorded each 10ms is connected to the low-voltage bus. This simulates, with high resolution, the dynamic behavior of the loads connected to the generator. **Figure 2** shows the real and reactive power response of a compressor with a rated power of 30 kW given a resistive pre-loading of 30 kW. Notice that the start-up time of the compressor takes around 12 s.


**Figure 1** Active and Reactive Power behavior for a 30 kW compressor load connection given a base load of 30 kW

On the generator side, the three-phase Synchronous Machine element is parametrized according to the information given by the manufacturer.

- **Rated Power (Prime Mover):** 0.3 MVA
- **Rated Voltage:** 400 V
- **Rated Power Factor:** 0.8
- **Connection:** Y
- **Inertia Constant H:** 0.6 s

Standard models for the frequency and voltage controller are initially selected based on the datasheet. Here, a first comparison against the available model variations is performed, to obtain the most likely suitable controller. In this work, the selected standard models are Woodward DEGOV and IEEE EXAC1, for frequency and voltage controller, respectively. A schematic of the composite model corresponding to the synchronous generator model is shown in **Figure 3**.

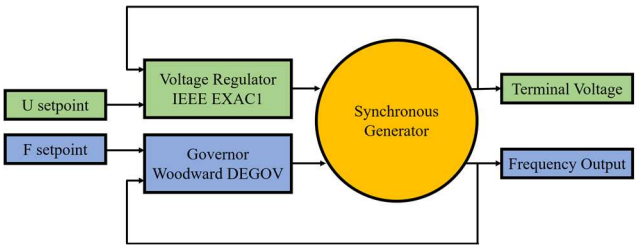


**Figure 3** Schematic of the simulation model of the diesel-electric generator

**Figures 4** and **5** illustrate the detailed models for the frequency and voltage controllers, respectively. DEGOV stands for diesel governor. It describes the mechanical power of a turbine driven by a diesel motor, responsible for inducing current on the generator side. This state-of-the-art governor is commonly used in the dynamical modeling of diesel-electric generators and two variations are known: with and without droop control. In this work, only one generator was considered, therefore, no droop is needed. EXAC1 stands for an excitation controller, whose power source is provided by the AC output of the same generator using non-controlled rectifiers like diodes.

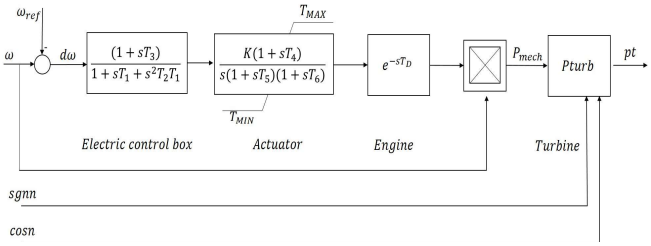


**Figure 4** Standard Woodward DEGOV Model [6]

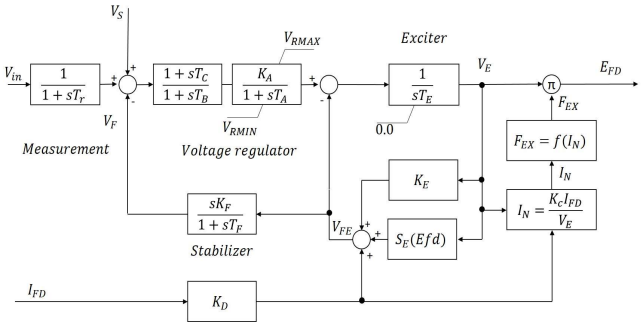


**Figure 5** Standard IEEE EXAC1 Model [2]

The Woodward diesel governor consists of the following main blocks: an electric speed sensor, a hydromechanical actuator, and the diesel engine itself, represented as a time delay. **Table 1** presents a detailed description of the physical meaning of all the variables defined in the model including their respective unit.

**Table 1** DEGOV Parameter Description

| Name | Description | Unit |
|---|---|---|
| $T_1$ | Governor mechanism time constant | s |
| $T_2$ | Turbine power time constant | s |
| $T_3$ | Turbine exhaust temperature time constant | s |
| K | Governor gain | pu |

| | | |
|---|---|---|
| $T_4$ | Governor lead time constant | s |
| $T_5$ | Governor lag time constant | s |
| $T_6$ | Actuator time constant | s |
| $T_d$ | Engine time delay | s |
| $T_{min}$ | Upper limit | pu |
| $T_{max}$ | Lower limit | pu |

The EXAC1 model comprises the following four main blocks: measurement, voltage regulator, exciter, and stabilizer. In contrast to the ten variables to be optimized on the selected governor model, the excitation control model consists of 17 variables, as described in **Table 2**.

**Table 2** EXAC1 Parameter Values

| Name | Description | Unit |
|---|---|---|
| $T_r$ | Voltage transducer filter | s |
| $T_b$ | Voltage regulator lag time constant | s |
| $T_c$ | Voltage regulator lead time constant | s |
| $K_a$ | Voltage regulator gain | pu |
| $T_a$ | Voltage regulator time constant | s |
| $V_{rmin}$ | Minimum voltage regulator output | pu |
| $V_{rmax}$ | Maximum voltage regulator output | pu |
| $T_e$ | Exciter time constant | s |
| $K_f$ | Stabilizer gain | pu |
| $T_f$ | Stabilizer time constant | s |
| $K_c$ | Rectifier loading factor | pu |
| $K_d$ | Demagnetizing factor | pu |
| E1 | Output voltage at which saturation is defined | pu |
| Se1 | Saturation value at the value E1 | pu |
| E2 | Output voltage at which saturation is defined | pu |
| Se2 | Saturation value at the value E1 | pu |
| $K_e$ | Exciter constant (self-excited field) | pu |

# 3 Methodology

This measurement-based approach counterbalances the physical significance of each parameter with its contribution to the output signals (e.g. frequency, voltage).
The data is acquired by stimulating the diesel generator with different base loads and load steps. The magnitude of the power jumps was defined considering a typical load step capability diagram of a diesel engine, which defines a fixed load acceptance value of 33% for base loads up to 67% [7]. The measurement data has been classified into four cases as shown in **Table 3**.

**Table 3** Load types cases

| Case Name | Load Type | Base load in kW | Power Jump in kW |
|---|---|---|---|
| Case a | Compressor | 30 | 30 |
| Case b | | 50 | |
| Case c | Resistive load bank | 20 | 20, 40 |
| Case d | | 60 | |

For the excitation controller, an initial comparison was performed considering the parameter range given by [2] with two standard sets found in [4] and [5]. An overview of these values can be found in **Table 4**.

**Table 4** EXAC1 Parameter Comparison

| Parameters | Parameter range [2] | Standard [4],[5] | Optimized |
|---|---|---|---|
| Tr [s] | 0 – 0.5 | 0 | 0.015 |
| Tb [s] | 0 – 20 | 0 | 0 |
| Tc [s] | 0 – 20 | 0 | 0 |
| Ka [-] | 0 – 1000 | 400 | 320 |
| Ta [s] | 0 – 10 | 0.02 | 0.012 |
| Vrmin [pu] | -10 – 0 | -5.43 | -4.0135 |
| Vrmax [pu] | 0 - 10 | 6.03 | 10 |
| Te [s] | 0.02 – 2 | 0.8 | 0.866 |
| Kf [pu] | 0 – 0.3 | 0.03 | 0.03 |
| Tf [s] | 0.02 – 1.5 | 1 | 1 |
| Kc [pu] | 0 – 1 | 0.2 | 0.1 |
| Kd [pu] | 0 – 1 | 0.38 | 0.00002 |
| E1 [pu] | - | 4.18 | 4.18 |
| Se1 [pu] | 0 – 1 | 0.1 | 0.1 |
| E2 [pu] | - | 3.14 | 3.14 |
| Se2 [pu] | 0 – 1 | 0.03 | 0.03 |
| Ke [pu] | 0 – 1 | 1 | 1 |

The application of an optimization algorithm at an early stage could lead to unnecessary long convergence time and not realistic results. Therefore, understanding the physical meaning of all the involved controller variables can be helpful for model simplification purposes, decreasing optimization algorithm convergence time and at the same time, obtaining plausible results.
The model validation in the case of the voltage controller was performed as illustrated in **Figure 6**.

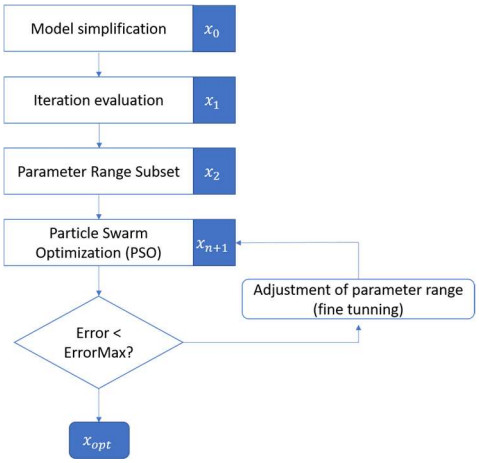


**Figure 6** Optimization algorithm

The starting point is a parameter set comprised by the defined range for each variable (**Table 4**) and denoted as $x_0$. This starting set has a dimension of seventeen rows and one

column whose content corresponds to the defined range for the corresponding variable.
During the model simplification stage, some variables were considered negligible or not to have a relevant influence on the voltage output. This is the case of the filter, the voltage regulator lag, and lead time constants, which were set to zero.
Since the magnitude of the load steps considered in this work was not significant enough to violate the saturation regions, all the variables on the saturation block were considered to be the same as standardly defined (E1, Se1, E2 and Se2). After this step, a parameter subset of $x_0$ is generated and named $x_1$. The dimension of the rows associated with a variable range is reduced to 10, as illustrated in Table 5.

**Table 5** Parameter Subset $x_1$ example

| Subset Name | Parameter Name | Parameter Value / Range | Status |
|---|---|---|---|
| $x_1$ | $T_r$ | 0 | fixed |
| | $T_b$ | 0 | fixed |
| | $T_c$ | 0 | fixed |
| | $K_a$ | 0 – 1000 | variable |
| | $T_a$ | 0 – 10 | variable |
| | $V_{rmin}$ | -10 – 0 | variable |
| | $V_{rmax}$ | 0 - 10 | variable |
| | $T_e$ | 0.02 – 2 | variable |
| | $K_f$ | 0 – 0.3 | variable |
| | $T_f$ | 0.02 – 1.5 | variable |
| | $K_c$ | 0 - 1 | variable |
| | $K_d$ | 0 - 1 | variable |
| | $E_1$ | 4.18 | fixed |
| | Se1 | 0.1 | fixed |
| | E2 | 3.14 | fixed |
| | Se2 | 0.03 | fixed |
| | $K_e$ | 0 - 1 | variable |

In the iteration evaluation stage, given all the remaining parameters and their respective fully defined range, iterations were performed on one variable simultaneously, leaving the other variables with the standard values defined in the literature. At the beginning, the precision of the iterations was directly connected to the defined parameter range. For instance, for variables like $K_c$ whose range is defined between zero and one, iterations every 0.1 pu were performed. In the same way, for variables like $V_{rmax}$ the iterations were performed every 1 pu since its defined range is between -10 and 0.
At the end of this stage, some parameter values were already fixed to a defined value, based on their proximity to the measurement data and the suggested standard values in [4] and [5]. The simulated most suitable value was selected based on a compromise between the peak magnitude (minimum, maximum) and its approximate time location when compared to the measurement data. At this point, the following variables found their best suitable value to be: $T_a$ at 0.015 s, $K_c$ at 0.2 pu, $K_e$ with 1 pu, $K_f$ fixed to 0.03 pu and $T_f$ equal to 1 s. The dimension of parameters (rows) associated with a variable range is now reduced to 5.
It is not a surprise that the remaining controller blocks have a high dynamical impact on the voltage output: voltage regulator ($K_a$, $V_{rmin}$ and $V_{rmax}$), exciter ($T_e$), and armature reaction ($K_d$). This parameter subset represents specific characteristics of the voltage regulator and exciter used by the manufacturer of the diesel generator.
The investigated range of these five variables was also shortened during the iteration evaluation stage. By this, a new parameter subset $x_2$ was generated, which contains all the shortened subranges from $x_1$ as well as all the fixed parameter values, that better approximate the measurement data. The subset $x_2$ is the initial input to the optimization algorithm phase.
Particle Swarm Optimization (PSO) algorithm was run for a considerably reduced number of parameters and their respective shortened range. In this stage, the measurement delay was again considered as an input to the optimization algorithm, to accurately reach the maximums and minimums in the voltage curve. The convergence time was also significantly reduced using the above-described procedure.
To evaluate whether an optimized value is accepted or discarded, the measurement data is compared with the results from a simulation using these optimized values by means of the mean square error (MSE), calculated as shown in Equation (1):

$$MSE = \frac{\sum(y_i - \hat{y}_i)^2}{n} * 100\ \% \qquad (1)$$

Being $y_i$ the simulated value, $\hat{y}_i$ the measurement value and $n$ the number of sampling points. In this work, a numerical comparison among other metrics like frequency minimum will also be presented in Section 4.
The PSO parameter range is continuously being reduced (updated) so that it better approximates the measurement data until the calculated error percentage is below the defined maximum value. The optimization algorithm ends and its output is a parameter set $x_{\text{opt}}$ which contains all the optimized values that best suit the measurement data. In this work, a threshold of 0.5% error was considered.
The model validation in the case of the frequency controller is similar to the case of the voltage regulator. The parameter range for the governor is given by [6] and standard sets were taken from [7]. An overview of these values can be found in **Table 6**.

**Table 6** DEGOV Parameter Comparison

| Parameters | Parameter range [6] | Standard [7] | Optimized |
|---|---|---|---|
| $T_1$ [s] | 0 - 25 | 0.2 | 0.001 |
| $T_2$ [s] | 0 – 0.5 | 0.1 | 0.000824 |
| $T_3$ [s] | 0 – 10 | 0.5 | 0.5 |
| K [pu] | 15 – 25 | 15 | 25 |
| $T_4$ [s] | 0 – 25 | 1 | 0.00451 |
| $T_5$ [s] | 0 – 10 | 0.1 | 0.099102 |

| | | | |
|---|---|---|---|
| $T_6$ [s] | 0 – 0.5 | 0.2 | 0.000006 |
| $T_d$ [s] | 0 – 0.125 | 0.01 | 0.01 |
| $T_{rmax}$ [pu] | 0 – 1.5 | 1.1 | 1.1 |
| $T_{rmin}$ [pu] | -0.05 – 0.5 | 0 | 0 |

The parameter set $x_0$, started with a dimension of ten rows (variable range). In the model simplification stage, we considered an ideal engine i.e. engine delay Td to be zero. Typical ignition delay is around 1 ms between 15% and 25% loading conditions. [8]
During the iteration evaluation stage, $T_{max}$, $T_{rmin,}$ and $T_3$ were set to their standard values since they had the best fit among the defined range.
Finally, the following parameter values were found using PSO: $T_1$, $T_2$, $T_4$, $T_5$, and $T_6$. Thus, reducing the optimization load to 60%. For the error evaluation, results generated with an engine time delay of 0.01 s were considered.
**Tables 4** and **6** include the resulting optimized parameter values for the voltage and frequency regulator, respectively. It is worth mentioning that although these parameter values were optimized for cases a and b, they are also valid for cases c and d, disregarding whether the load was connected or disconnected from the generator (positive or negative load steps). At the end of Section 4, an evaluation of the error percentage obtained for all cases in **Table 3** is shown.

# 4 Results

The results section is divided into four test cases.

## 4.1 Test Case I: Comparison with standard values

**Figure 7** shows a comparison between measurement and simulation data, using standard and optimized controller values. The data correspond to the same 30 kW compressor load connection at t = 10 s shown in **Figure 2**.

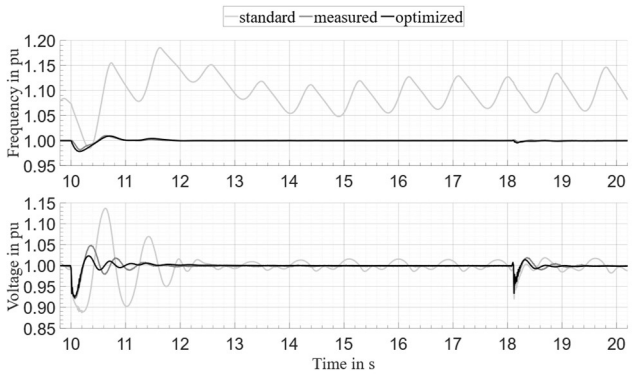


**Figure 7** Comparison between measured and simulated frequency and voltage response after the connection of a 30 kW compressor

The optimized curves are best suited to the measured values for the frequency and voltage outputs. It is clear that results obtained from the standard controller values do not correlate with the measurement data. This lack of correlation could lead to wrong conclusions when a deeper analysis is performed.

## 4.2 Test Case II: Resistive-Inductive load connection

**Figure 8** shows a comparison of the frequency and voltage response among cases a and b, which correspond to the connection of a 30 kW compressor given a base load of 30 kW and 50 kW respectively. As shown in **Figure 2**, the start-up of the compressor contains two transient curves one at t = 10 s and the second around t =18 s. These two moments in time are shown on the left and right sides of **Figure 8,** respectively.

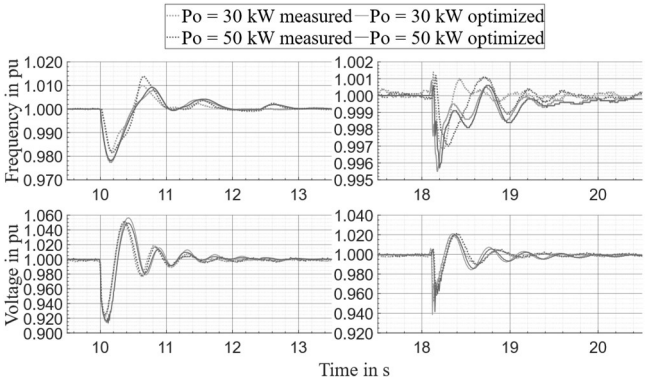


**Figure 8** Comparison between measured and simulated response of the generator model, for the connection of a compressor load ΔP = 30 kW given two different base loads

It can be noted that although the base load is different for these two cases, the frequency dip is very similar when a resistive-inductive load is connected to the generator. The simulated model is able to replicate accurately the dynamics of the nadir frequency. In the case of the rate of change of the frequency (RoCoF), a relatively high error between the measurement and simulation value is evident, which could be explained by the error calculation procedure, since it takes the complete file of measurement data including the connection and disconnection of the load and not the gradient(s) separated from each other. The consideration of the RoCoF could be a further extension of this work., as shown in **Table 7**.

**Table 7** Overview of frequency properties for cases a, b

| **Case Name / frequency property** | **Case a** | **Case b** |
|---|---|---|
| Measurement Nadir frequency (Hz) | 49.09 | 49.07 |
| Simulated Nadir frequency (Hz) | 48.87 | 48.90 |
| Measurement RoCoF at 100ms (Hz/s) | -7.65 | -7.30 |
| Simulated RoCoF at 100ms (Hz/s) | -9.75 | -9.50 |

On the voltage side, the maximums and minimums, oscillatory behavior, and damping times after the resistive-inductive load connection are also accurately replicated. A similar detailed numerical analysis as **Table 7** could be performed for the voltage output characteristics.

## 4.3 Test Case III: Base load Influence for resistive-only load connection

**Figures 9** and **10** show a comparison of the frequency and voltage response between cases c and d, respectively. This corresponds to an additional load connection of 20 kW and 40 kW, given a base load of 20 kW and 60 kW, correspondingly.

For both base loading cases, a load step of the same magnitude has a similar effect on both frequency dips. But as expected, for higher base loads (case d), a deeper load connection produces a deeper nadir frequency and requires a longer recovery time.

Although the predicted RoCoF of the validated model is higher than the measured one, in the analysis under consideration it is desired that the simulation results provide a higher margin of confidence than expected in practice.

Similar effects due to the load stepping can be identified on the voltage curve, i.e. deeper voltage peaks for deeper power jumps. All transient oscillations are damped after 1 s of the load event. These effects are also replicated by the validated simulation model as shown in **Table 8**.

**Table 8** Overview of frequency properties for case c (base load 20 kW)

| Case Name / frequency property (P0=20 kW) | ΔP=20 kW | ΔP=40 kW |
|---|---|---|
| Measurement Nadir frequency (Hz) | 49.69 | 49.39 |
| Simulated Nadir frequency (Hz) | 49.61 | 49.25 |
| Measurement RoCoF at 100ms (Hz/s) | -2.15 | -4.60 |
| Simulated RoCoF at 100ms (Hz/s) | -2.80 | -5.55 |

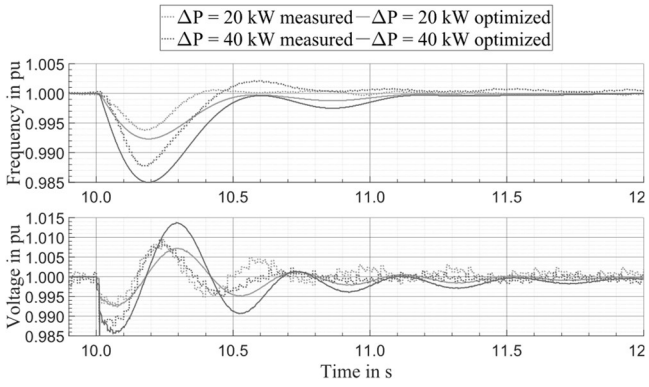


**Figure 9** Comparison between simulated and measured response of the generator model, for the connection of additional load given a base load of 20 kW (case c)

**Table 9** Overview of frequency properties for case d (base load 60 kW)

| Case Name / frequency property (P0 = 60 kW) | ΔP=20 kW | ΔP=40 kW |
|---|---|---|
| Measurement Nadir frequency (Hz) | 49.60 | 49.09 |
| Simulated Nadir frequency (Hz) | 49.61 | 49.14 |
| Measurement RoCoF at 100ms (Hz/s) | -2.55 | -7.10 |
| Simulated RoCoF at 100ms (Hz/s) | -3.05 | -7.60 |

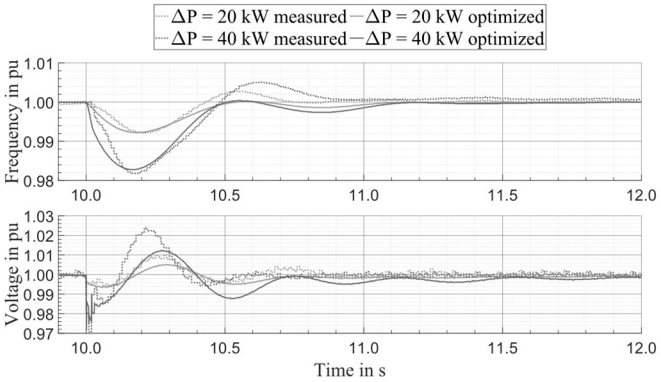


**Figure 10** Comparison between simulated and measured response of the generator model, for the connection of additional load given a base load of 60 kW (case d)

## 4.4 Test Case IV: Load Step Influence for resistive-only load connection

**Figure 11** shows a comparison of the frequency and voltage response considering a power jump of 20 kW for two different base loads. In **Figure 12**, a load step of 40 kW is considered. Similar to Test Case II, the base load plays a minor role in the measured nadir frequency. It can be stated that the frequency and voltage dips are mainly depending on the magnitude of the power step, as expected. The higher the additional load connection, the deeper the drops in the voltage and frequency response will be.

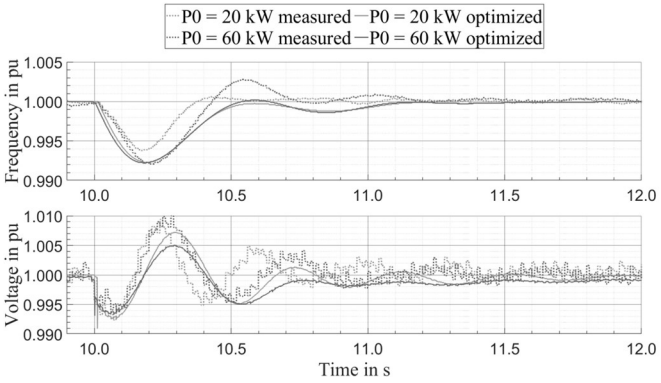


**Figure 11** Comparison between the simulated and measured response of the generator model, for the connection of additional 20 kW load, given different base loads

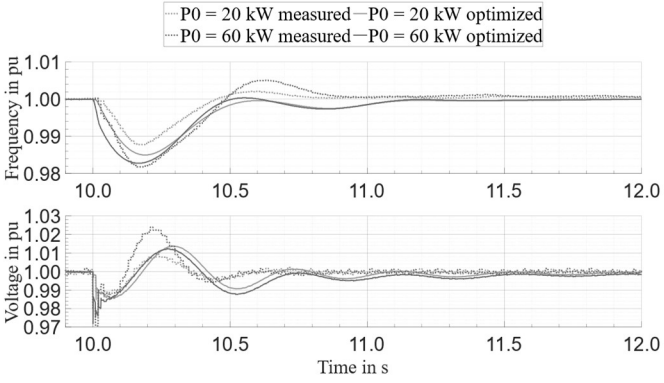


**Figure 12** Comparison between the simulated and measured response of the generator model, for the connection of additional 40 kW load, given different base loads

No clear mathematical relationship could be established between different base loads and the frequency dynamics, nevertheless, a higher base load could be associated with a higher frequency gradient.

Finally, an overview of the mean square error percentage obtained on each load case is shown in **Figure 13**. The error between measurement data and optimized simulation data was compared to the error between measurement data and standard simulation data. The comparison of cases c and d included both load steps (ΔP=20 kW and ΔP=40 kW) as described in **Table 3**. The highest error percentages were obtained on the frequency output. Results obtained with standard parameters are up to 70 times far away from the ones with a validated model for the case of the frequency and up to 90 times for the case of the voltage.

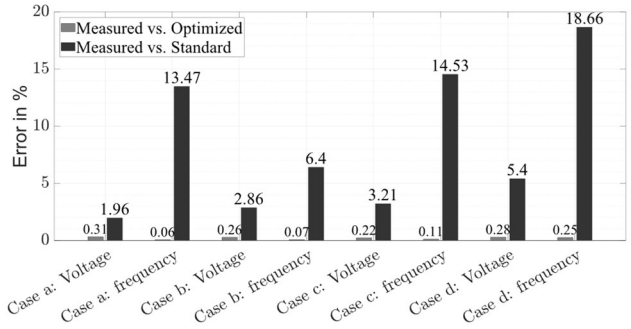


**Figure 13** Comparison between simulated and measured values of frequency and voltage of the generator model

# 5 Conclusions

This work proposed a general methodology for parameter identification using standard controller models of a diesel-electric generator and measurement data.

Starting with a high number of parameters to be optimized on the governor and excitation regulators, an initial simplification is performed considering the background understanding of the functionality of each block inside the controller. The main blocks influencing the voltage output are the voltage regulator, exciter, and armature reaction. In the case of the frequency output, is the actuator box as shown in previous works [9]. A shortened iteration range contributes to a shorter convergence time and better performance of the optimization algorithm. Finally, defining a maximum error level is important to increase the accuracy of the validated simulation model.

The results section showed that it is possible to find a set of optimized parameter values using the proposed methodology without significant loss of its reliability. A trustworthy approximation for the frequency and voltage outputs could be obtained through a range of parameter values valid for all the tested events in this work.

It is important to state that although the optimized parameter values are valid for all the defined load cases, the existence of a different set of parameter values valid for higher load steps is plausible. Nevertheless, the load step capability of the diesel engine should also be considered. To extend the validity range of the validated model beyond the tested cases in this work, a non-linear parametrization of the controller would be necessary.

# 6 References


[1] T. Petermann et al., "What happens during a blackout (in german: Was bei einem Blackout geschieht)" in Studien des Büros für Technikfolgen-Abschätzung beim Deutschen Bundestag – 33, 2011.

[2] "Exciter Models" Standard Dynamic Excitation Systems in NEPLAN Power System Analysis Tool. Web Address: https://www.neplan.ch/wp-content/uploads/2015/08/Nep_EXCITERS1.pdf (14.03.2023)

[3] I. C. Report "Excitation System Models for Power System Stability Studies" in IEEE Transactions on Power Apparatus and Systems, vol. PAS-100, no. 2, pp: 494-509, Feb. 1981, DOI: 10.1109/TPAS.1981.316906

[4] P. Kundur, "Excitation Systems" in Power System Stability and Control, 1st ed., USA: Mc Graw Hill, 1993, pp. 347-364.

[5] "Recommended Practice for Excitation System Models for Power System Stability Studies" in IEEE Std 421.5-2016 (Revision of IEEE Std 421.5-2016, vol., no., pp. 1-207, 26 Aug. 2016, DOI: 10.1109/IEESTD.2016.7553421

[6] "Turbine Governor Models" Standard Dynamic Turbine Governor Systems in NEPLAN Power System Analysis Tool. Web Address: https://www.neplan.ch/wp-content/uploads/2015/08/Nep_TURBINES_GOV.pdf (18.05.2023)

[7] S. Sommerville, G. Taylor and M. Abbod, "Frequency Stability Considerations of Reciprocating Gas Engine Generators in Microgrids", presented at the 2021 56th Universities Power Engineering Conference (UPEC) DOI: 10.1109/UPEC50034.2021.9548254

[8] M. Mustayen, X. Wang, M. Rasul, J. Hamilton, M. Negnevitsky, "Thermodynamic analysis of diesel engine ignition delay under low load conditions", presented at the 8th International Conference on Energy and Environment Research ICEER 2021, DOI: 10.11016/j.egyr.2022.01.201

[9] C. Lin, C. Wu, J. Yang and C. Liao, "Parameters identification of reduced governor system model for diesel-engine generator by using hybrid particle swarm optimization", IET Electr. Power Appl., 2018, Vol. 12 Iss. 9, pp. 1265-1271, DOI: 10.1049/iet-epa.2017.0851

[10] C. Shah et al., "High-Fidelity Model of Stand-Alone Diesel Electric Generator with Hybrid Turbine-Governor Configuration for Microgrid Studies", IEEE Access Volume 10, 2022, DOI: 10.1109/ACCESS.2022.3211300

[11] P. P. Leza, "Transient Study in Diesel Synchronous Generator", Ph. D. Dissertation, Universidad de Oviedo, 2017.



Supported by:

Federal Ministry for Economic Affairs and Climate Action

on the basis of a decision by the German Bundestag